JOURNAL OF Applied Polymer SCIENCE

Optorheological Thickening Under the Pulsed Laser Photocrosslinking of a Polymer

Stephen Richard Okoniewski,[1] Danielle Wisniewski,[2] N. Laszlo Frazer,[1] Weiqiang Mu,[1] Andrew Arceo,[3] Pranjali Rathi,[3] J. B. Ketterson[1,4]

[1]Department of Physics and Astronomy, Northwestern University, Evanston Illinois 60208
[2]Department of Chemistry, Northwestern University, Evanston Illinois 60208
[3]Adlai E. Stevenson High School, Lincolnshire Illinois 60069
[4]Department of Electrical Engineering and Computer Science, Northwestern University, Evanston Illinois 60208
Correspondence to: N. L. Frazer (E-mail: japs@laszlofrazer.com)

ABSTRACT: Electro-, magneto-, and other rheological effects can be used to externally control fluid viscosity. However, they are largely reversible and in addition subject to colloidal settling, electrostatic breakdown, or high cost. In the experiments described here the dependence of the viscosity of a polymer solution under pulsed laser photocrosslinking as a function of radiation dose is determined using the Brownian motion of colloidal polystyrene tracers that were optically confined to a one dimensional channel. The system studied was a transparent aqueous solution of poly(ethylene glycol) dimethacrylate together with a 1-hydroxycyclohexyl phenyl ketone photoinitiator. An increase in the viscosity of the solution with the laser fluence was observed. The growth was exponential, stable between pulses, and spanned nearly three orders of magnitude. © 2014 Wiley Periodicals, Inc. J. Appl. Polym. Sci. **2014**, *131*, 40690.

KEYWORDS: crosslinking; irradiation; kinetics; viscoelasticity; viscosity

Received 21 January 2014; accepted 7 March 2014
DOI: 10.1002/app.40690

INTRODUCTION

The manipulation of rheological properties is an important aspect of the study of complex fluids. Effects studied include compositional changes, shear (as in jamming[1] and non-Newtonian fluids[2,3]), electrorheological,[4,5] magnetorheological,[6] and thermorheological[7] responses. Some applications call for remotely controlled, stable increases in viscosity. Microrheology has been shown to be an effective tool for monitoring abrupt gellation in photopolymerizing monomers.[8] Here, we describe the stable thickening of a polymer solution under successive doses of ultraviolet light as it is monitored through the Brownian motion of microscopic polystyrene tracer beads.

The optical manipulation of the mechanical properties of polymers is a useful, established means of fabrication. Photopolymerization and crosslinking can be used to print 3D structures[9] and as a negative resist in 2D lithography.[10] They are also used for in-place moldable repairs, for example in dentistry.[11,12] Investigations of the crosslinking process itself are important for developing higher contrast, more sensitive photopolymers.[13] Examples of existing tools to measure the propagation of radicals produced by a pulsed laser in a polymer solution include size-exclusion chromatography[14,15] and electron paramagnetic resonance.[16]

Here, we report in situ measurements of the combined local viscosity of a polymer solution as hydrogel formation[17] is in progress by monitoring the diffusion of dielectric colloidal tracers in the solution. Poly(ethylene glycol) dimethacrylate (PEGDMA) was chosen as the base unit in this experiment due to its hydrophilic nature, transparency, and ability to photocrosslink using UV light and an appropriate photoinitiator.[18,19] The PEGDMA/water ratio used in this experiment was designed to be transparent, allowing the tracers to be tracked with a microscope as photocrosslinking doses were applied. The mean square displacement of the tracers after a time t (1/30 second in the present case),

$$\langle x^2 \rangle = 2Dt \tag{1}$$

was used to determine the one-dimensional diffusion constant, D.

Under some circumstances the presence of Brownian motion can complicate the imaging and assembly of structures from colloidal particles. Typically, this is resolved with confocal microscopy[20,21]; however, this is a slow process if multiple particles are to be tracked. In this study, Brownian motion was restricted to one dimension by creating a two dimensional optical trap[22–24] within the solution. The trap confined the particles to the imaging region while leaving the solution itself undisturbed. This type of trap has

facilitated studies of one dimensional electromagnetic[25] and hydrodynamic[26] properties. It has also allowed for the experimental investigation of single file diffusion.[27–29] In this experiment, the trap allowed us to measure particle motion in the plane imaged by the microscope.

In our trap, one direction of confinement arises from radiation pressure, which pushes the particles against the far wall of the container. Hydrodynamic interactions with the wall can introduce small systematic errors.[30] In the most confined geometry previously reported,[30] viscosity measurements deviated from the bulk value by a factor of one third. We use a relatively thick cell relative to our tracer size to reduce this error. Wall effects in an optical trap are less significant than those found in fully enclosed microfluidic trap.[31] The second trapping dimension arises from the steep intensity gradient associated with the interference between two incoming coherent laser beams. The beams enter symmetrically about the axis of a focusing lens and subsequently form an in-plane standing wave at the container wall, as we describe below. Particles were trapped in the bright constructive interference maxima. The steepness of the potential was controlled by the fringe spacing as well as the intensities and relative coherence of the two beams, both of which can be controlled. There was a weak optical trapping force in the third direction on the scale of the laser spot size at the sample. The parameters of the optical potential in this type of trap can be rapidly altered.

Diffusion along the third axis was in the horizontal plane, so density (mis)match[32] did not require consideration. The viscosity of the photocrosslinking solution was determined from the one dimensional diffusion constant using the Stokes-Einstein equation

$$D = k_B T/(6\pi\eta r) \quad (2)$$

where η is the viscosity, T is the temperature (293 Kelvin in the present case), and r is the radius of the tracer particle. In addition to impacting the diffusion constant, temperature can influence polymer degredation, termination, and autoacceleration.[16] This approach makes the approximations that the fluid is Newtonian and not viscoelastic.

EXPERIMENTAL

Solution Development

The crosslinking process used in these experiments was a simplification of the one used by DiRamio et al.[33] They used both PEGDMA and monoalkene PEGMA polymers. PEG polymers are crosslinked by irradiation of the alkene terminator, so we used only bialkene PEGDMA with an average molecular weight of 550. 1-Hydroxycyclohexyl phenyl ketone (1.17 g/mL) was used as a photoinitiator. Both were obtained from Sigma-Aldrich. Carboxylate modified polystyrene microspheres with a diameter of 1.1 μm (2% solids), azide (2 m*M*), and water solution were obtained from Molecular Probes for use as a tracer.

To observe the evolution of the viscosity through imaging, a low viscosity, transparent, selectively photocrosslinking solution was developed. A 90% by volume PEGDMA/10% water/0.1% photoinitiator/0.1% tracer solution was found to excessively scatter light. The solution was subsequently diluted with water.

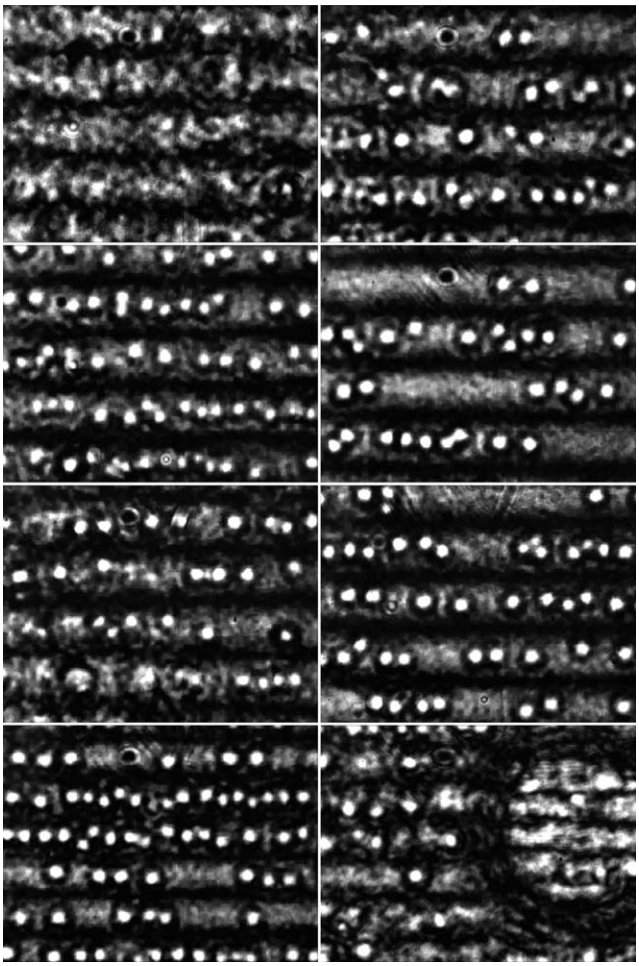

Figure 1. Images of the solution with tracers and interference fringes from the optical trap present. Water volume fractions are 10%, 18%, 25%, 31%, 36%, 40%, 44%, and 47% left to right and then top to bottom. Image quality improves until the polymer and water begin to separate in the final image. Each image is 15 μm wide.

Optical quality thereby improved until separation of the water and polymer onset at about 45% water (Figure 1).

For the photocrosslinking experiment, samples were prepared by dissolving 10 mg of initiator in 700 μL of pure water, then adding 800 μL of PEGDMA, and finally adding 5 nL of tracer. The mixture was then sonicated for 5 min to improve homogeneity. This colloidal solution has good transparency, relatively low viscosity (not distinguishable from water), is stable under exposure to the 532 nm trapping laser (or room lighting), and readily photocrosslinks into a hydrogel when exposed to 325 nm from the crosslinking laser.

Sample cells were made from two microscope cover slips which sandwich a piece of 0.1 mm thick double sided sticky tape which had been hole punched. The hole was filled with solution before the top cover slip was pressed down to seal the cell (Figure 2).

Optics

Trapping. A diagram of the optical trapping and photocrosslinking system is shown in Figure 3. The trap interferometer

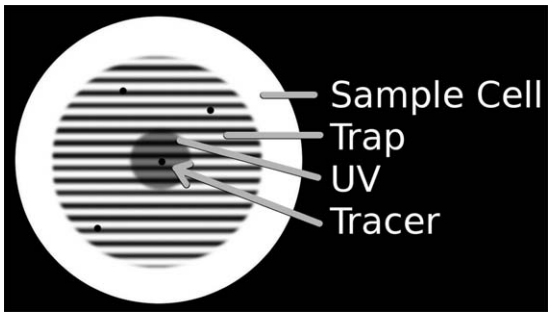

Figure 2. Top view diagram of a sample cell. The trap and UV beams enter the cell from the top. Differences in scale between features are greatly understated for clarity.

optics began with an intracavity doubled Nd:YVO_4 532 nm, 300 mW continuous wave laser. The 532 nm beam was first sent through a beam expander (L1, L2), which was adjustable through translation of L2. This determined the overall size of the optical lattice. The beam was split (BS) by a 50 : 50 nonpolarizing beam splitter. These beams were sent along two different paths.

The top path is composed of three mirrors, two of which were mounted on a translatable stage. Translating this stage changed the length of the top path, which in turn changed the standing wave ratio of the subsequent optical lattice due to the coherence length of the laser. Fringe visibility was greatest when the path lengths of the two beams were equal. The bottom path was just composed of two mirrors.

Both beams were then directed onto a right angle mirror. The reflected pair of parallel beams was sent into a 500 nm dichroic shortpass filter which served as a beam combiner (BC). The 532 nm beams struck BC at a 45° angle and underwent 95% reflectance into a fused silica 50 mm lens (L4); the beams arrived symmetrically on each side of the lens's axis. The beams were subsequently focused together to form a standing wave interference pattern in the sample (S).

The angle between the converging beams was adjustable by translating the right angle mirror, which changed the distance between the beams at L4. Typically, it was between 5° and 25°,

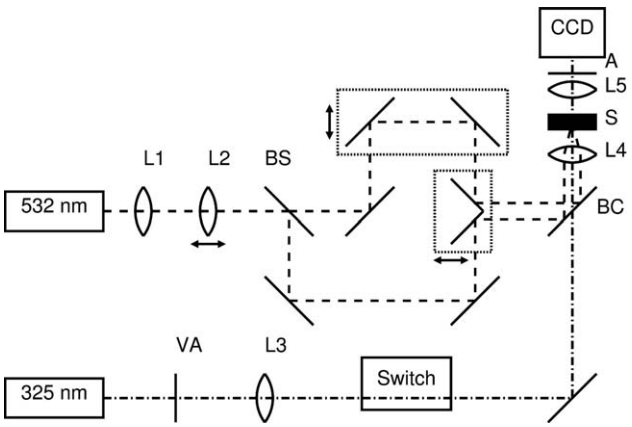

Figure 3. Diagram of optical equipment for laser trapping and crosslinking.

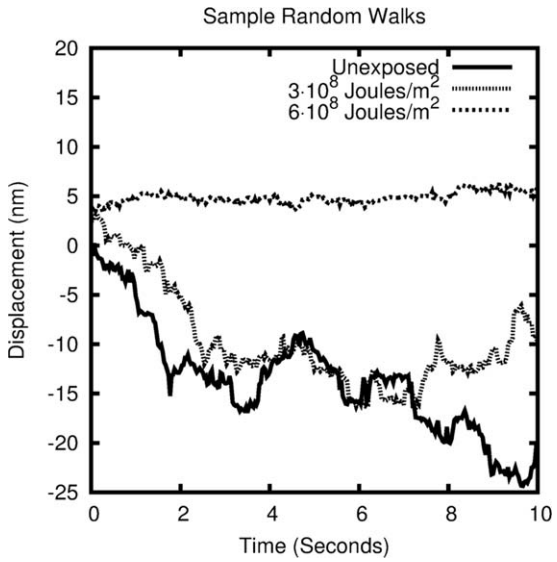

Figure 4. Examples of random walks of the tracer particle through solution with varying degrees of exposure to crosslinking ultraviolet radiation. Unexposed solution shows the most particle mobility. Doubling the ultraviolet dose produces a dramatic reduction in particle motion because viscosity increases exponentially with dose.

leading to interference fringe wavelengths between 5 μm and 1 μm. The optical trap confined the tracer spheres in two dimensions over a large area with a radius of about 0.7 mm.

Crosslinking. The output of the 325 nm HeCd crossliking laser passed through a variable attenuator and subsequently through 1 m fused silica lens which reduced the beam diameter (L3). The beam was pulsed for 50 ms using an electrically controlled shutter formed by fastening an extension to the arm of a conventional electrical relay. Around 92% of the 325 nm beam's intensity was transmitted by BC at 45° incidence and was focused into the optical trap by L4. The 325 nm beam power was measured between L4 and S. The beam spot radius at the sample was 0.1 mm, which was much larger than the tracer size and much smaller than the trap area or sample area, allowing for repeated crossliking experiments with a single sample simply by translating the stage to expose unmodified solution.

Imaging. A 100× 0.9 NA microscope objective (L5) magnified and recollimated the light which passed through the sample. The sample and an interference pattern were imaged, after attenuation (A) of the laser to reduce brightness, with a 30 frames per second CCD camera. Only the 532 nm laser light was detected. 30 s videos of single tracers were recorded after each laser pulse. An isolated particle in each video was tracked. Examples of one dimensional random walks are shown in Figure 4. Ten trials were averaged to determine the viscosity.

RESULTS AND DISCUSSION

Previous studies conducted on the properties of photocrosslinked PEGDMA found that as the percent water in the hydrogel increased, the hydrogel undergoes a polymerization induced phase separation process.[18,34] In this work, we observed similar traits, as shown in Figure 1, with the phase separation process

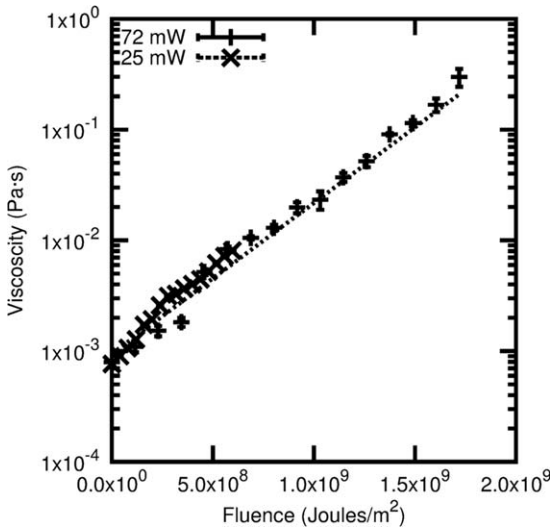

Figure 5. Solution viscosity increases with 325 nm laser fluence. The curve is Eq. (3).

seen at ~53% PEDGMA/47% water. The polymer solution ratios described in the experimental selection were chosen to ensure minimal viscosity to avoid excessive light scattering and to ensure phase separation has not yet occurred. By making use of an optical trap, the change in viscosity as a function of polymerization of the polymer solution was studied with the appropriate polymer/water ratio. For future studies, a lower molecular weight base unit could be used to decrease the viscosity while allowing for a higher polymer to water ratio.

The viscosity determined through particle tracking for two different laser powers is shown in Figure 5. Importantly, the viscosity did not evolve between laser pulses. The measured relationship between viscosity and fluence ϕ was

$$\eta = 9\times10^{-4}\times e^{\left(\frac{\phi}{3\times10^{8}\,\mathrm{Joules/m}}\right)}\,\mathrm{Pa}\times\mathrm{s} \qquad (3)$$

Particle tracking and associated software allowed precise subpixel measurements. The smallest value in this study was about $\sqrt{x^2}=10$ nm, or 1/3 of a pixel. Imaging was assisted using an optical trap to maintain tracers in the overall field of view without limiting the local diffusion in one dimension.

CONCLUSIONS

A quantitative, rapid in situ measurement of the optorheological thickening effect in low cost PEGDMA has been demonstrated. It is observed that the viscosity increases under precisely controlled laser pulsing. Unlike conventional rheological effects, viscosity is manipulated from a distance in optorheological thickening. Particle tracking measurements of photopolymerization of acrylate resins showed a sudden step in the mean squared particle displacement as a function of dose, indicative of a sharp phase transition from liquid to a gel with essentially infinite viscosity. The dose threshold depended on the solution composition and the penetration of the radiation through the sample.[8] In this experiment, the viscosity change is gradual and dose controllable. The simple rheological behavior could be surprising considering that the transport of the crosslinking alkene terminators is inhibited by higher viscosities.[16] Unlike other rheological effects, such as jamming and the electrorheological effect, the viscosity increase does not reverse but remains stable. The fluid used was transparent and selectively thickened when illuminated with 325 nm, but not when illuminated with visible light.

We note that the techniques developed may be of interest to the polymer community more generally, beyond our demonstration in a model hydrogel system. A readily implemented improvement would be to shorten the time scales over which measurements can be made by imaging bead fluctuations onto a four quadrant photodiode where the wider bandwidths can lead to much shorter times for determining the local viscosity.[26] If sufficiently short time scales are measured, viscoelasticity and non-Newtonian flow could also be investigated.[35]

ACKNOWLEDGMENTS

The authors gratefully acknowledge support by the NU-MRSEC REU/RET program, NSF DMR-1121262, NSF IGERT DGE-0801685, and ISEN. They thank Wesley Burghardt and Eric Brown for helpful discussions.

REFERENCES

1. Trappe, V.; Prasad, V.; Cipelletti, L.; Segre, P. N.; Weitz, D. A. *Nature* **2001**, *411*, 772.
2. Brown, E.; Jaeger, H. M. *Phys. Rev. Lett.* **2009**, *103*, 086001.
3. Poslinski, A. J. *J. Rheol.* **1988**, *32*, 703.
4. Ruzicka, M. Electrorheological Fluids: Modeling and Mathematical Theory; Springer: Berlin, **2000**; p 1748.
5. Wen, W.; Huang, X.; Yang, S.; Lu, K.; Sheng, P. *Nat. Mater.* **2003**, *2*, 727.
6. Ashour, O.; Rogers, C. A.; Kordonsky, W. *J. Intell. Mater. Syst. Struct.* **1996**, *7*, 123.
7. Wood-Adams, P.; Costeux, S. *Macromolecules* **2001**, *34*, 6281.
8. Slopek, R. P.; McKinley, H. K.; Henderson, C. L.; Breedveld, V. *Polymer* **2006**, *47*, 2263.
9. Cumpston, B.; Ananthavel, S.; Barlow, S. *Nature* **1999**, *398*, 51.
10. Lorenz, H.; Despont, M.; Fahrni, N.; LaBianca, N.; Renaud, P.; Vettiger, P. *J Micromech. Microeng.* **1999**, *7*, 121.
11. Stansbury, J. W. *J. Esthet. Dent.* **2000**, *12*, 300.
12. Dickens, S. H.; Stansbury, J. W.; Choi, K. M.; Floyd, C. J. E. *Macromolecules* **2003**, *36*, 6043.
13. Cruise, G. M.; Hegre, O. D.; Scharp, D. S.; Hubbell, J. A. *Biotechnol. Bioeng.* **1998**, *57*, 655.
14. Beuermann, S.; Buback, M.; Davis, T. P.; Gilbert, R. G.; Hutchinson, R. A.; Olaj, O. F.; Russell, G. T.; Schweer, J.; Van Herk, A. M. *Macromol. Chem. Phys.* **1997**, *198*, 1545.
15. Van Herk, A. M. *J. Macromol. Sci. Part C Polym. Rev.* **1997**, *37*, 633.
16. Andrzejewska, E. *Prog. Polym. Sci.* **2001**, *26*, 605.
17. Pusey, P. N.; Pirie, A. D.; Poon, W. C. K. *Phys. A* **1993**, *201*, 322.

18. Killion, J. A.; Geever, L. M.; Devine, D. M.; Kennedy, J. E.; Higginbotham, C. L. *J. Mech. Behav. Biomed. Mater.* **2011**, *4*, 1219.
19. Zhang, K.; Simon, C. G.; Washburn, N. R.; Antonucci, J. M.; Lin-Gibson, S. *Biomacromolecules* **2005**, *6*, 1615.
20. Burke, M. D.; Park, J. O.; Srinivasarao, M.; Khan, S. A. *J. Control. Release* **2005**, *104*, 141.
21. Kramer, E. M.; Frazer, N. L.; Baskin, T. I. *J. Exp. Bot.* **2007**, *58*, 3005.
22. Mu, W.; Wang, G.; Luan, L.; Spalding, G.; Ketterson, J. B. *New J. Phys.* **2006**, *8*, 70.
23. Mu, W.; Li, Z.; Luan, G.; Spalding, G.; Wang, G.; Ketterson, J. B. *JOSA B* **2008**, *25*, 763.
24. Rohner, J.; Fournier, J.-M.; Jacquot, P.; Merenda, F.; Salathe, R. P. *Proc. SPIE* **2006**, *15*, 632606.
25. Burns, M. M.; Fournier, J.-M.; Golovchenko, J. A. *Phys. Rev. Lett.* **1989**, *63*, 1233.
26. Meiners, J.-C.; Quake, S. R. *Phys. Rev. Lett.* **1999**, *82*, 2211.
27. Lutz, C.; Kollmann, M.; Bechinger, C. *Phys. Rev. Lett.* **2004**, *93*, 026001.
28. Lutz, C.; Kollmann, M.; Leiderer, P.; Bechinger, C. *J. Phys. Condens. Matter* **2004**, *16*, S4075.
29. Wei, Q.-H.; Bechinger, C.; Leiderer, P. *Nature* **2000**, *287*, 625.
30. Faucheux, L. P.; Libchaber, A. *J. Phys. Rev. E* **1994**, *49*, 5158.
31. Sato, J.; Breedveld, V. *J. Rheol.* **2006**, *50*, 1.
32. Aarts, D. G. A. L.; Van der Wiel, J. H. ; Lekkerkerker, H. N. W. *J. Phys.: Condens. Matter* **2002**, *15*, S245.
33. Diramio, J. A.; Kisaalita, W. S.; Majetich, G. F.; Shimkus, J. M. *Biotechnol. Prog.* **2005**, *21*, 1281.
34. Kang, G.; Cao, Y.; Zhao, H.; Yuan, Q. *J. Membr. Sci.* **2008**, *318*, 227.
35. Mason, T.; Ganesan, K.; van Zanten, J.; Wirtz, D.; Kuo, S. *Phys. Rev. Lett.* **1997**, *79*, 3282.